

Poles of Karlsruhe-Helsinki KH80 and KA84 solutions extracted by using the Laurent+Pietarinen method

Alfred Švarc*

Rudjer Bošković Institute, Bijenička cesta 54, P.O. Box 180, 10002 Zagreb, Croatia

Mirza Hadžimehmedović, Rifat Omerović, Hedim Osmanović, and Jugoslav Stahov
University of Tuzla, Faculty of Science, Univerzitetska 4, 75000 Tuzla, Bosnia and Herzegovina

(Dated: April 2, 2014)

Poles of partial wave scattering matrices in hadron spectroscopy have recently been established as a sole link between experiment and QCD theories and models. Karlsruhe-Helsinki (KH) partial wave analyses have been “above the line” in the Review of Particle Physics (RPP) for over three decades. The RPP compiles Breit-Wigner (BW) parameters from local BW fits, but give only a limited number of pole positions using speed plots (SP). In the KH method only Mandelstam analyticity is used as a theoretical constraint, so these partial wave solutions are as model independent as possible. They are a valuable source of information. It is unsatisfactory that BW parameters given in the RPP have been obtained from the KH80 solution, while pole parameters have been obtained from the KA84 version. To remedy this, we have used a newly developed Laurent+Pietarinen expansion method to obtain pole positions for all partial waves for KH80 and KA84 solutions. We show that differences from pole parameters are, with a few exceptions, negligible for most partial waves. We give a full set of pole parameters for both solutions.

PACS numbers: 11.55Bq, 11.55Fv, 14.20Gk

* alfred.svarc@irb.hr

I. INTRODUCTION

Revisions to the Review of Particle Physics (RPP) [1] and contributions to recent workshops [2–4] have emphasized that poles, rather than Breit-Wigner parameters, quantify resonance masses and widths and make a link between scattering theory and QCD. It appears that Karlsruhe-Helsinki partial wave analyses make one of the most reliable data analyses “above the line” in the RPP [1] for almost three decades, and give Breit-Wigner parameters over local energy ranges. The pole parameters are given for only some of them. They are presently extracted from speed plots (SP) as described by Höhler in [5–7]. Let W be the center of mass energy. In Ref. [5] it was shown that by using $SP(W) = |dT(W)/dW|$, and T -matrices defined as $T(W) = T_b + R\Gamma e^{i\phi}/(M - W - i\Gamma/2)$ where T_b is background term, methods of Ref. [6] are inadequate because the phase information is not obtained. Reference [5] proposed an improvement by introducing Argand plots for $dT(W)/dW$. This work assumed that $dT_b(W)/dW$ can be neglected. This succeeded for several partial waves, but not all. Auxiliary assessments were recommended; 4-star resonances were derived from speed plots and Argand diagrams dT/dW over the range $W = M \pm \Gamma/2$. The locations of $T(M)$ and $T(M \pm \Gamma/2)$ in the Argand plot for $T(W)$ were calculated by interpolating the partial wave solution KA84. Next, the radius R and phase ϕ were used to fit the resonance loop, assuming that background T_b is constant over the range $W = M \pm \Gamma/2$. The expressions $\tilde{T}(M)$ and $\tilde{T}(M \pm \Gamma/2)$ denote points calculated for parameters R and ϕ . It is shown that $T(M)$ and $\tilde{T}(M)$ agree using this construction; however values $T(M \pm \Gamma/2)$ and $\tilde{T}(M \pm \Gamma/2)$ are in general not yet quite satisfactory. Therefore Γ , R and ϕ were adjusted until a good fit was obtained. This procedure was successful for eight of the 4-star resonances, and the parameters are listed in Table 1 of Ref. [5]. This Table, based on the KA84 solution, is now cited in the RPP as KH pole positions.

In summary, the SP method is actually a three step procedure: i) make a classic speed plot; ii) make an Argand plot for $dT(W)/dW$ and establish a phase ϕ ; iii) correct Γ , R and ϕ so that the interpolated value of KH (or any other) amplitude and Argand plot coincide. We repeat the description of this procedure in detail because some younger colleagues use only the first step because Höhler’s references [5] and [6] are not easily accessible.

This opens two issues: i) is the generalized SP method able to find all poles in KH amplitudes? And secondly; ii) are SP pole parameters obtained from KH80 solution comparable with the pole position from KA84? So, the question arises: “How similar these two solutions are?” Here we answer both issues.

Regarding issue i) we use the newly developed Laurent+Pietarinen method (L+P method) [8, 9] to extract all visible poles from KH80 and KA84 solutions. Differences between these solutions are quantified here.

Regarding issue ii), it is known from [5, 7] that these two solutions are not drastically different, but are definitely not identical.

As other analyses have shown that the SP method is only a first order approximation of more general search methods [10, 11], it remains a mystery to us why other methods have not been used to complete the fragmentary list of KH pole parameters obtained by using SP technique only.

So, the main purpose of this paper is to remedy these problems. We use the recent Laurent+Pietarinen (L+P) method [8, 9] to extract pole positions from both KH80 and KA84 solutions. We show figures and pole parameters for both, and compare them. We find more poles than originally established by the SP technique, and confirm that differences between the two sets of KH solutions are negligible. All results agree well with present results displayed in the RPP [1].

II. FORMALISM

A. Two classic partial wave analyses

For almost three decades two significantly different partial wave analyses have appeared “above the line” in the RPP: the Carnegie-Mellon-Berkeley (CMB) analysis of Cutkosky et al. [12–14], and the Karlsruhe-Helsinki analysis by Höhler et al. [15]. These two analyses enforce slightly different criteria. The CMB model [12–14] produced partial wave poles directly, but had some problems with Breit-Wigner parameters [14]. The Karlsruhe-Helsinki approach was much more successful in stabilizing solutions, but had some problems in extracting BW parameters and poles.

1. CMB model

Ref. [12] amalgamated and stabilized the data base; in Ref. [13] they performed a single-energy stabilized partial wave analysis, and in Ref. [14] developed a global solution; a coupled-channel model with analyticity and unitarity explicitly included which they use to fit partial wave data of Ref. [13]. They explicitly get partial wave poles by analytic continuation into the complex energy plane, but have some problems defining an “analog” to BW parameters. They do not make a local BW fit, but use their coupled-channel model to extract BW parameters. Their list of BW parameters and poles is complete.

2. KH80 method

The KH80 method used a different approach. Instead of performing energy stabilization at the level of partial waves, they evaluated pion-nucleon invariant amplitudes using forward dispersion relations and the Pietarinen expansion. The stabilization method is close to model independent. The only constraint used is Mandelstam analyticity. The method includes amplitude analysis at fixed t , amplitude analysis at fixed cm angles, backward amplitude analysis and ordinary energy independent partial wave analysis, all of them linked into one computer program.

The fixed- t amplitude analysis used C^\pm , and B^\pm invariant amplitudes over a large angular domain in the range $-1 \leq t(\text{GeV}^2) \leq 0$; invariant amplitudes satisfy exact fixed- t analyticity and $s - u$ crossing symmetry. Data are available up to lab. momentum $k = 200\text{GeV}/c$.

The analysis at fixed c.m. scattering angle was done at 18 angles with $-0.8 \leq \cos\theta \leq +0.8$. Forward and backward amplitude analyses were performed separately [15].

Energy independent partial wave analysis is the third step in the Karlsruhe method. Partial waves were fitted to data and to invariant amplitudes at fixed- t , fixed c.m. scattering angle, backward and forward at the same momentum and energy. The strength of the constraints was adjusted allowing the possibility of weak resonances. Partial waves found in one iteration were used to reconstruct invariant amplitudes iteratively. The whole method converged in several iterations [15].

The final step in the KH method was to fit partial waves to experimental data. For that reason partial waves from KH80 partial wave analysis are only approximately smooth as a function of energy. A smoother solution KA84 [16] was constructed from KH80 work using constraints from s-channel partial wave dispersion relations, fixed-s dispersion relations and information from the nearby part of the Mandelstam double spectral function [17].

Being almost model independent and consistent with Mandelstam analyticity, the Karlsruhe-Helsinki partial wave solutions are a valuable input for extraction of resonances in the πN system. We use data from the original KH code preserved by one of our collaborators (Jugoslav Stahov¹) from Tuzla.

B. Laurent (Mittag-Leffler) expansion

We generalize the Laurent expansion to the Mittag-Leffler theorem [9, 18], which expresses a function in terms of its first k poles and an entire function:

$$T(W) = \sum_{i=1}^k \frac{a_{-1}^{(i)}}{W - W_i} + B^L(W); \quad a_{-1}^{(i)}, W_i, W \in \mathbb{C}. \quad (1)$$

Here, W is c.m. energy, $a_{-1}^{(i)}$ and W_i are residues and pole positions for the i -th pole, and $B^L(W)$ is a function regular in all $W \neq W_i$. It is important to note that this expansion is not a representation of the unknown function $T(W)$ in the full complex energy plane, but is restricted to the part of the complex energy plane where the expansion converges. If we choose poles as expansion points, the Laurent series converges on the open annulus around each pole.

¹ Jugoslav Stahov was one of the original “KH task force” members.

The outer radius of the annulus extends to the position of the next singularity (such as a nearby pole). Our Laurent expansion converges on a sum of circles located at the poles, and this part of the complex energy plane in principle includes the real axes. By fitting the expansion (1) to the experimental data on the real axis, this in principle gives exact values of s -matrix poles.

The novelty of our approach is a particular choice for the non-pole contribution $B^L(W)$, based on an expansion method used by Pietarinen for πN elastic scattering.

Before proceeding, we briefly review this method.

C. Pietarinen series

A specific type of conformal mapping technique was proposed and introduced by Ciulli [19, 20] and Pietarinen [21], and used in the Karlsruhe-Helsinki partial wave analysis [15] as an efficient expansion of invariant amplitudes. It was later used by a number of authors to solve problems in scattering and field theory [22], but not applied to the pole search prior to our recent study [9]. A more detailed discussion of the use of conformal mapping and this method can be found in Refs.[9, 18].

If $F(W)$ is a general unknown analytic function with a cut starting at $W = x_P$, it can be represented as a power series of “Pietarinen functions”

$$F(W) = \sum_{n=0}^N c_n X(W)^n, \quad W \in \mathbb{C}$$

$$X(W) = \frac{\alpha - \sqrt{x_P - W}}{\alpha + \sqrt{x_P - W}}, \quad c_n, x_P, \alpha \in \mathbb{R}, \quad (2)$$

with α and c_n acting as tuning parameter and coefficients of the Pietarinen function $X(W)$ respectively.

The essence of the approach is that $(X(W)^n, n = 1, \infty)$ forms a complete set of functions defined on the unit circle in the complex energy plane with a branch cut starting at $W = x_P$; the analytic form of the function is initially undefined. The final form of the analytic function $F(W)$ is obtained by introducing a rapidly convergent power series with real coefficients, and the degree of the expansion is automatically determined by fitting the input data. In the calculation of Ref. [21], as many as 50 terms were used; in the present analysis, covering a narrower energy range, fewer terms are required.

D. Application of Pietarinen series to scattering theory

The analytic structure of each partial wave is well known. Every partial wave contains poles which parameterize resonant contributions, cuts in the physical region starting at thresholds of elastic and all possible inelastic channels, plus t -channel, u -channel and nucleon exchange contributions quantified with corresponding negative energy cuts. However, the explicit analytic form of each cut contribution is not known. Instead of guessing the exact analytic form of all of these, we use one Pietarinen series to represent each cut, and the number of terms in the Pietarinen series is determined by the quality of fit to the input data. In principle we have one Pietarinen series per cut; branch points $x_P, x_Q \dots$ are known from physics, and coefficients are determined by fitting the input data. In practice, we have too many cuts (especially in the negative energy range), so we reduce their number by dividing them into two categories: all negative energy cuts are approximated with only one, effective negative energy cut represented by one (Pietarinen) series (we denote its branch point as x_P), while each physical cut is represented by a separate series with branch points determined by the physics of the process ($x_Q, x_R \dots$).

In summary, the set of equations which define the Laurent expansion + Pietarinen series method (L+P method) is:

$$\begin{aligned}
T(W) &= \sum_{i=1}^k \frac{a_{-1}^{(i)}}{W - W_i} + B^L(W) \\
B^L(W) &= \sum_{n=0}^M c_n X(W)^n + \sum_{n=0}^N d_n Y(W)^n + \sum_{n=0}^N e_n Z(W)^n + \dots \\
X(W) &= \frac{\alpha - \sqrt{x_P - W}}{\alpha + \sqrt{x_P - W}}; \quad Y(W) = \frac{\beta - \sqrt{x_Q - W}}{\beta + \sqrt{x_Q - W}}; \quad Z(W) = \frac{\gamma - \sqrt{x_R - W}}{\gamma + \sqrt{x_R - W}} + \dots \\
&\quad a_{-1}^{(i)}, W_i, W \in \mathbb{C} \\
&\quad c_n, d_n, e_n, \alpha, \beta, \gamma \dots \in \mathbb{R} \text{ and } x_P, x_Q, x_R \in \mathbb{R} \text{ or } \mathbb{C} \\
&\quad \text{and } k, M, N \dots \in \mathbb{N}.
\end{aligned} \tag{3}$$

As our input data are on the real axes, the fit is performed only on this dense subset of the complex energy plane. All Pietarinen parameters in equations (3) are determined by the fit.

We observe that the class of input functions which may be analyzed with this method is quite wide. One may either fit partial wave amplitudes obtained from theoretical models, or possibly experimental data directly. In either case, the T -matrix is represented by this set of equations (3), and minimization is usually carried out in terms of χ^2 .

E. Real and complex branch points

Branch points $x_P, x_Q, x_R \dots$ in the Pietarinen expansion (3) can be real or complex. However, real or complex branch points describe different physical situation. If the branch points $x_P, x_Q, x_R \dots$ are real numbers, this means that our background contributions are defined by stable initial and final state particles. Then all contributions to the observed processes are created by intermediate isobar resonances, and all other initial and final state contributions are given by stable particles, as described by Pietarinen expansions with real branch point coefficients. From experience we know that this in principle is not true: a three body final state is always created provided that the energy balance allows for it, and in three body final states we typically do have a contribution from one stable particle (nucleon or pion), and many other combinations of two-body resonant substates like $\sigma, \rho, \Delta \dots$. So we choose the model where the first two branch points x_P and x_Q are always real, but the third branch point x_R can be either real (two body final states) or complex (three body final state with a resonance in a two body subsystem).

Let us claim the fact that single channel character of the method prohibits us to establish with certainty which mechanism prevails. Using data from a single channel only (the existing KH80 and KA84 input) we are unable with certainty to say whether the new resonant state which appears is an isobar state with two body final states, or a three body final state with a resonance in a two body subsystem. If only single channel information is available, we have two alternatives: either we obtain a good fit with an extra resonance and stable initial and final state particles (real branch points), or we obtain a good fit with one resonance less, and a complex branch point. Data from a single channel data does not distinguish between the two. This effect has been already spotted, elaborated and discussed in the case of Jülich model, and a more detailed elaboration how the ρN complex branch point interferes and intermixes with $P_{11}(1710) 1/2^+$ [23, 24].

Issues connected with importance of inelastic channels, and two-body resonant sub-states in three-body final states have already been recognized in Ref. [5] (paragraphs 4.2 and 4.3). However, at that time, a formalism to follow and quantify these effects didn't exist, so no estimates have been given. L+P formalism with complex branch points enables us to study these effects in detail.

1. In either case, a new resonant state is established, but our single-channel method cannot say where (either in two body intermediate state or in three-body subchannel). We cannot distinguish whether the new resonant state manifests itself as a new isobar resonance with stable initial and final states (real branch points), or as a resonance in two-body subchannel of three-body final state (complex branch point). For that, we need the data from extra channels, and an experiment giving us missing information on ratio of 2-body/3-body cross sections at the same energies is badly missing.

The advantage of the Pietarinen expansion method is that it can be extended directly to complex branch points; we using it to search for suspicious partial waves.

2. We claim that this effect is not affecting only $P_{11}(1710)$ resonance as established by the Jülich group [23, 24] for the ρN branch point, but influences interpretation of many more resonances from the RPP (at least we have established that for the Karlsruhe-Helsinki PWA). One definitely needs measurements from other channels before claiming whether the observed structure is an intermediate isobar resonance, or a resonance appearing in the two-body subsystem of a three body final state. Single channel measurements are insufficient, we need multi-channel measurements in order to distinguish between the two. Höhler has in his Newsletter's paper [5] discussed similar problems, but he blamed guilt on the ωN branch point. However, in this paper we claim the effects of the ρN branch point are much more pronounced. We have tested the influence of the better known $\pi\Delta$ branch point located at $(1370 - 140)$ MeV on KH amplitudes, but as it is much lower in mass than the ρN branch point, its influence was negligible.

F. Fitting procedure

We use three Pietarinen functions (one with a branch point in the unphysical region to represent all left-hand cuts, and two with branch points in the physical region to represent the dominant inelastic channels), combined with the minimal number of poles. We also allow the possibility that one of the branch points becomes a complex number allowing all three-body final states to be effectively taken into account. We generally start with 5 Pietarinen terms per decomposition, and the anticipated number of poles. The discrepancy criteria are defined below using a discrepancy parameter D_{dp} . This quantity is minimized using MINUIT and the quality of the fit is visually inspected by comparing fitting function with data. If the fit is unsatisfactory (discrepancy parameters are too high, or fit visually does not reproduce the fitted data), the number of Pietarinen terms is increased, and if it does not help, the number of poles is increased by one. The fit is repeated, and the quality of the fit is re-estimated. This procedure is continued until we reach a satisfactory fit.

Pole positions, residues, and Pietarinen coefficients α , β , γ , c_i , d_i and e_i are our fitting parameters. However, in the strict spirit of the method, Pietarinen branch points x_P , x_Q and x_R should not be fitting parameters; each known cut should be represented by its own Pietarinen series, fixed to known physical branch points. While this would be ideal, in practice the application is somewhat different. We can never include all physical cuts from the multi-channel process.

Instead, we represent them by a smaller subset. So, in our method, Pietarinen branch points x_P , x_Q and x_R are not generally constants; we have explored the effect of allowing them to vary as fitting parameters. In the following, we shall demonstrate that when searched, the branch points in the physical region still naturally converge towards branch points which belong to channels which dominate a particular partial wave, but may not actually correspond to them exactly. The proximity of the fit results to exact physical branch points describes the goodness of fit; it tells us how well certain combinations of thresholds is indeed approximates a partial wave. Together with the choice of the degree of Pietarinen polynomial, this represents the model dependence of our method. We do not claim that our method is entirely model independent. However, the method chooses the simplest function with the given analytic properties which fit the data, and increases the complexity of the function only when the data require it.

G. Error analysis

When we fit KH80 and KA84 amplitudes, we have to define which parameters we are minimizing.

For both solutions we introduce the discrepancy parameter per data point D_{dp} (the substitute for χ^2_{dp} per data point when analyzing experimental data):

$$D_{dp} = \frac{1}{2N_{data}} \sum_{i=1}^{N_{data}} \left[\left(\frac{\text{Re}T_i^{fit} - \text{Re}T_i^{KH}}{Err_i^{\text{Re}}} \right)^2 + \left(\frac{\text{Im}T_i^{fit} - \text{Im}T_i^{KH}}{Err_i^{\text{Im}}} \right)^2 \right], \quad (4)$$

where N_{data} is the number of energies, and errors of KH80 and KA84 solutions are introduced as:

$$\begin{aligned}
Err_i^{\text{Re}} &= 0.05 \frac{\sum_{k=1}^{N_{data}} |\text{Re}T_k^{KH}|}{N_{data}} + 0.05 |\text{Re}T_i^{KH}| \\
Err_i^{\text{Im}} &= 0.05 \frac{\sum_{k=1}^{N_{data}} |\text{Im}T_k^{KH}|}{N_{data}} + 0.05 |\text{Im}T_i^{KH}|.
\end{aligned} \tag{5}$$

When errors of the input numbers are not given, and one wants to make a minimization, errors have to be estimated. There are two simple ways to do it: either assigning a constant error to each data point, or introducing an energy dependent error as a percentage of the given value. Both definitions have drawbacks. For the first recipe only high-valued points are favored, while in the latter case low-valued points tend to be almost exactly reproduced. We find neither satisfactory, so we follow prescriptions used by GWU and Mainz groups, and use a combined error which consists of a sum of constant and energy dependent errors.

In our principal paper [9] we have tested the validity of the model on a number of well known πN amplitudes, and concluded that the method is very robust. That paper did not present an error analysis. That is done here.

In the L+P method we have statistical and systematic uncertainties: 1. statistical; and 2. systematic.

1. Statistical uncertainty

Statistical uncertainties are simply taken from MINUIT, which is used for minimization. It is shown separately in all tables as the first term.

2. Systematic uncertainty

Systematic uncertainty is the error of the method itself, and requires a more detailed explanations.

Our Laurent decomposition contains only two branch points in the physical region, and this is far from enough in a realistic case. Any realistic analytic function in principle contains more than two branch points approximated in our model by a different analytic function containing only two.

We use the following procedure to define systematic uncertainties:

- i) We release the first (unphysical) branch point x_P because we have no control over background contributions;
- ii) We always keep the first physical branch point x_Q fixed at $x_Q = 1077$ MeV (the πN threshold).
- iii) The error analysis is done by varying the remaining physical branch point x_R in two ways:
 - 1. We fix the third branch point x_R to the threshold of the dominant inelastic channel for the chosen partial wave (e.g. the η threshold for S-wave) if only one inelastic channel is important, or in case of several equally important inelastic processes we perform several runs with the x_R branch point fixed to each threshold in succession.
 - 2. We release the third branch point x_R allowing MINUIT to find an effective branch point representing all inelastic channels. If only one channel is dominant, the result of the fit will be close to the dominant inelastic channel.
- iv) We average results of the fit, and obtain the standard deviation.

The choice of all values for the branch point x_R is given in the Appendix (Tables VI for KH80 solution and Table VII for KA84). The quality of our fits for both KH80 and KA84 solutions are measured by the discrepancy parameter D_{dp} defined in Eqs. (4) and (5).

III. RESULTS

A. Real branch points

In Tables I - IV and in Figs. 1 - 4 we show L+P pole parameters and quality of the fit for all KH80 and KA84 partial waves for the case where the reaction is 2-body \rightarrow 2-body with an unknown number of

resonances in intermediate isobar states. In Tables VI and VII, given in the Appendix, we show corresponding L+P parameters. In this case three-body final states are neglected.

TABLE I. Pole positions in MeV and residues of partial waves as moduli in MeV and phases in degrees for lowest $I = 1/2$ partial waves. The results from L+P expansion are given for Karlsruhe-Helsinki 80 (KH80) and Karlsruhe 84 (KA84) analysis. Resonances marked with a star indicate resonances which can be explained by the ρN complex branch point. RPP denotes the range of pole parameters given by Ref. [1], and RPP H93 denotes the values of pole parameters named HOEHLER 93 in the RPP, and taken from RPP and Table 1 of Ref. [5].

PW	Source	Resonance	$\text{Re } W_p$	$-2\text{Im } W_p$	$ \text{residue} $	θ
S_{11}	RPP		1490 – 1530	90 – 250	50 ± 20	(−15 ± 15)°
	RPP H93		1487	–	–	–
	KH80 L+P	$N(1535) 1/2^-$	$1509 \pm 4 \pm 2$	$118 \pm 9 \pm 2$	$22 \pm 2 \pm 0.4$	$(-5 \pm 5 \pm 3)^\circ$
	KA84 L+P		$1505 \pm 3 \pm 1$	$103 \pm 7 \pm 3$	$20 \pm 2 \pm 1$	$(-14 \pm 3 \pm 1)^\circ$
	RPP		1640 – 1670	100 – 175	20 – 50	(−50 – 80)°
	RPP H93		1670	163	39	−37°
	KH80 L+P	$N(1650) 1/2^-$	$1660 \pm 3.5 \pm 1$	$167 \pm 8 \pm 2$	$47 \pm 3 \pm 1$	$(-47 \pm 3 \pm 1)^\circ$
	KA84 L+P		$1663 \pm 3 \pm 0$	$165 \pm 7 \pm 1$	$45 \pm 2 \pm 1$	$(-44 \pm 3 \pm 1)^\circ$
	RPP		1900 – 2150	90 – 479	1 – 60	(0 – 164)°
	RPP H93		–	–	–	–
	KH80 L+P	$N(1895) 1/2^-$	$1917 \pm 19 \pm 1$	$101 \pm 36 \pm 1$	$3.1 \pm 1.4 \pm 0$	$(-107 \pm 23 \pm 2)^\circ$
	KA84 L+P		$1920 \pm 19 \pm 2$	$93 \pm 15 \pm 3$	$2.7 \pm 1 \pm 0.2$	$(-105 \pm 23 \pm 3)^\circ$
P_{11}	RPP		1350 – 1380	160 – 220	40 – 52	(−75 – 100)°
	RPP H93		1385	164	40	–
	KH80 L+P	$N(1440) 1/2^+$	$1363 \pm 2 \pm 2$	$180 \pm 4 \pm 5$	$50 \pm 1 \pm 2$	$(-88 \pm 1 \pm 2)^\circ$
	KA84 L+P		$1365 \pm 2 \pm 4$	$187 \pm 4 \pm 10$	$48 \pm 1 \pm 3$	$(-88 \pm 1 \pm 4)^\circ$
	RPP		1670 – 1770	80 – 380	6 – 15	(90 – 200)°
	RPP H93		1690	200	15	–
	KH80 L+P	$N(1710)^* 1/2^+$	$1770 \pm 5 \pm 2$	$98 \pm 8 \pm 5$	$5 \pm 1 \pm 1$	$(-104 \pm 7 \pm 3)^\circ$
	KA84 L+P		$1763 \pm 4 \pm 9$	$105 \pm 5 \pm 10$	$6 \pm 1 \pm 1$	$(-117 \pm 4 \pm 15)^\circ$
	RPP		2120 ± 40	180 – 420	14 ± 7	(35 ± 25)°
	RPP H93		–	–	–	–
	KH80 L+P	$N(2100)^* 1/2^+$	$2052 \pm 6 \pm 3$	$337 \pm 10 \pm 4$	$30 \pm 1 \pm 1$	$(-92 \pm 3 \pm 2)^\circ$
	KA84 L+P		$2023 \pm 5 \pm 25$	$346 \pm 9 \pm 13$	$32 \pm 1 \pm 3$	$(-118 \pm 3 \pm 21)^\circ$
P_{13}	RPP		1660 – 1690	150 – 400	15 ± 8	(−130 ± 30)°
	RPP H93		1686	187	15	–
	KH80 L+P	$N(1720) 3/2^+$	$1677 \pm 4 \pm 1$	$184 \pm 8 \pm 1$	$13 \pm 1 \pm 0$	$(-115 \pm 3 \pm 2)^\circ$
	KA84 L+P		$1685 \pm 4 \pm 1$	$178 \pm 8 \pm 1$	$13 \pm 1 \pm 1$	$(-104 \pm 4 \pm 1)^\circ$
	RPP		1870 – 1930	140 – 300	3 ± 2	(10 ± 35)°
	RPP H93		–	–	–	–
	KH80 L+P	$N(1900)^* 3/2^+$	$1928 \pm 18 \pm 2$	$152 \pm 40 \pm 9$	$4 \pm 1 \pm 1$	$(-29 \pm 15 \pm 2)^\circ$
	KA84 L+P		$1920 \pm 17 \pm 1$	$215 \pm 37 \pm 2$	$7 \pm 1 \pm 1$	$(-38 \pm 11 \pm 1)^\circ$

B. Complex branch points

In Table V we give the parameters for some typical situations when fits with complex branch points achieve the similar quality as fits with the real ones (measured by the size of discrepancy variable D_{dp} , see Eq. 4). The complex branch point is a mathematical implementation of the situation when the three-body final state contains a two body sub-channel accompanied by the third “observer” particle. In this case we also allow for an extra resonance in the subchannel, but it is not located in the isobar intermediate state, but in the final state interaction. Both mechanisms (real and complex branch points) are indistinguishable in a single channel model. As was the case in the Jülich model for $P_{11}(1710)$, other channels (in the Jülich model KA channel) are essential to distinguish between the two.

TABLE II. Pole positions in MeV and residues of partial waves as moduli in MeV and phases in degrees for higher $I = 1/2$ partial waves. The results from L+P expansion are given for Karlsruhe-Helsinki 80 (KH80) and Karlsruhe 84 (KA84) analysis. Resonances marked with a star indicate resonances which can be explained by ρ N complex branch point. RPP denotes the range of pole parameters given by Ref. [1], and RPP H93 denotes the values of pole parameters named HOEHLER 93 in RPP, and taken over from RPP and Table 1 of Ref. [5].

PW	Source	Resonance	$\text{Re } W_p$	$-2\text{Im } W_p$	residue	θ
D_{13}	RPP		1505 – 1515	105 – 120	35 ± 3	(−10 ± 5)°
	RPP H93		1510	120	32	−8°
	KH80 L+P	$N(1520) \ 3/2^-$	$1506 \pm 1 \pm 1$	$115 \pm 2 \pm 1$	$33 \pm 1 \pm 1$	$(-15 \pm 1 \pm 1)^\circ$
	KA84 L+P		$1506 \pm 1 \pm 1$	$116 \pm 2 \pm 2$	$33 \pm 1 \pm 1$	$(-15 \pm 1 \pm 1)^\circ$
	RPP		1650 – 1750	100 – 350	5 – 50	(−120 to 20)°
	RPP H93		1700	120	5	–
	KH80 L+P	$N(1700)^* \ 3/2^-$	$1757 \pm 4 \pm 1$	$136 \pm 7 \pm 4$	$7 \pm 1 \pm 1$	$(-113 \pm 4 \pm 2)^\circ$
	KA84 L+P		$1743 \pm 4 \pm 4$	$132 \pm 7 \pm 2$	$7 \pm 1 \pm 1$	$(-134 \pm 4 \pm 6)^\circ$
	RPP		1800 – 1950	150 – 250	2 – 10	(180 ± 80)°
	RPP H93		–	–	–	–
D_{15}	KH80 L+P	$N(1875)^* \ 3/2^-$	$2094 \pm 7 \pm 11$	$296 \pm 15 \pm 4$	$13 \pm 1 \pm 1$	$(-2 \pm 4 \pm 9)^\circ$
	KA84 L+P		$2120 \pm 6 \pm 11$	$270 \pm 13 \pm 5$	$11 \pm 1 \pm 1$	$(17 \pm 4 \pm 5)^\circ$
	RPP		1655 – 1665	125 – 150	25 ± 5	(−25 ± 6)°
	RPP H93		1656	126	23	−22°
	KH80 L+P	$N(1675) \ 5/2^-$	$1654 \pm 2 \pm 0$	$125 \pm 3 \pm 1$	$23 \pm 1 \pm 0$	$(-25 \pm 2 \pm 0)^\circ$
	KA84 L+P		$1656 \pm 1 \pm 0$	$123 \pm 2 \pm 1$	$23 \pm 1 \pm 0$	$(-23 \pm 1 \pm 1)^\circ$
	RPP		2100 ± 60	360 ± 80	20 ± 10	(−90 ± 50)°
	RPP H93		–	–	–	–
	KH80 L+P	$N(2060)^* \ 5/2^-$	$2119 \pm 11 \pm 1$	$370 \pm 20 \pm 5$	$19 \pm 1 \pm 1$	$(-94 \pm 5 \pm 1)^\circ$
	KA84 L+P		$2134 \pm 9 \pm 5$	$352 \pm 18 \pm 7$	$18 \pm 1 \pm 1$	$(-80 \pm 4 \pm 2)^\circ$
F_{15}	RPP		1665 – 1680	110 – 135	40 ± 5	(−10 ± 10)°
	RPP H93		1673	135	44	−17°
	KH80 L+P	$N(1680) \ 5/2^+$	$1674 \pm 2 \pm 1$	$129 \pm 3 \pm 1$	$44 \pm 1 \pm 1$	$(-16 \pm 1 \pm 1)^\circ$
	KA84 L+P		$1672 \pm 2 \pm 1$	$132 \pm 4 \pm 1$	$45 \pm 2 \pm 1$	$(-16 \pm 2 \pm 1)^\circ$
	RPP		2030 ± 110 or 1779	480 ± 100 or 248	10 – 115	(−100 ± 40)°
	RPP H93		–	–	–	–
	KH80 L+P	$N(2000)^* \ 5/2^+$	$1834 \pm 19 \pm 6$	$122 \pm 34 \pm 7$	$4 \pm 1 \pm 1$	$(-39 \pm 18 \pm 9)^\circ$
	KA84 L+P		$1838 \pm 20 \pm 25$	$182 \pm 40 \pm 25$	$5 \pm 2 \pm 1$	$(-39 \pm 20 \pm 27)^\circ$
	RPP		2050 – 2100	400 – 520	30 – 72	(−30 to 30)°
	RPP H93		2042	482	45	–
G_{17}	KH80 L+P	$N(2190) \ 7/2^+$	$2079 \pm 4 \pm 9$	$509 \pm 7 \pm 16$	$54 \pm 1 \pm 3$	$(-18 \pm 1 \pm 3)^\circ$
	KA84 L+P		$2065 \pm 3 \pm 11$	$526 \pm 7 \pm 2$	$59 \pm 1 \pm 1$	$(-22 \pm 1 \pm 5)^\circ$
G_{19}	RPP		2150 – 2250	350 – 550	20 – 30	(−50 ± 30)°
	RPP H93		2187	388	21	–
	KH80 L+P	$N(2250) \ 9/2^-$	$2157 \pm 3 \pm 14$	$412 \pm 7 \pm 44$	$24 \pm 1 \pm 5$	$(-62 \pm 1 \pm 11)^\circ$
	KA84 L+P		$2187 \pm 3 \pm 4$	$396 \pm 6 \pm 19$	$22 \pm 1 \pm 2$	$(-41 \pm 1 \pm 3)^\circ$
H_{19}	RPP		2130 – 2200	400 – 560	33 – 60	(−45 ± 25)°
	RPP H93		2135	400	40	−50°
	KH80 L+P	$N(2220) \ 9/2^+$	$2127 \pm 3 \pm 24$	$380 \pm 7 \pm 22$	$38 \pm 1 \pm 5$	$(-52 \pm 1 \pm 14)^\circ$
	KA84 L+P		$2139 \pm 3 \pm 3$	$390 \pm 6 \pm 1$	$41 \pm 1 \pm 1$	$(-48 \pm 1 \pm 1)^\circ$

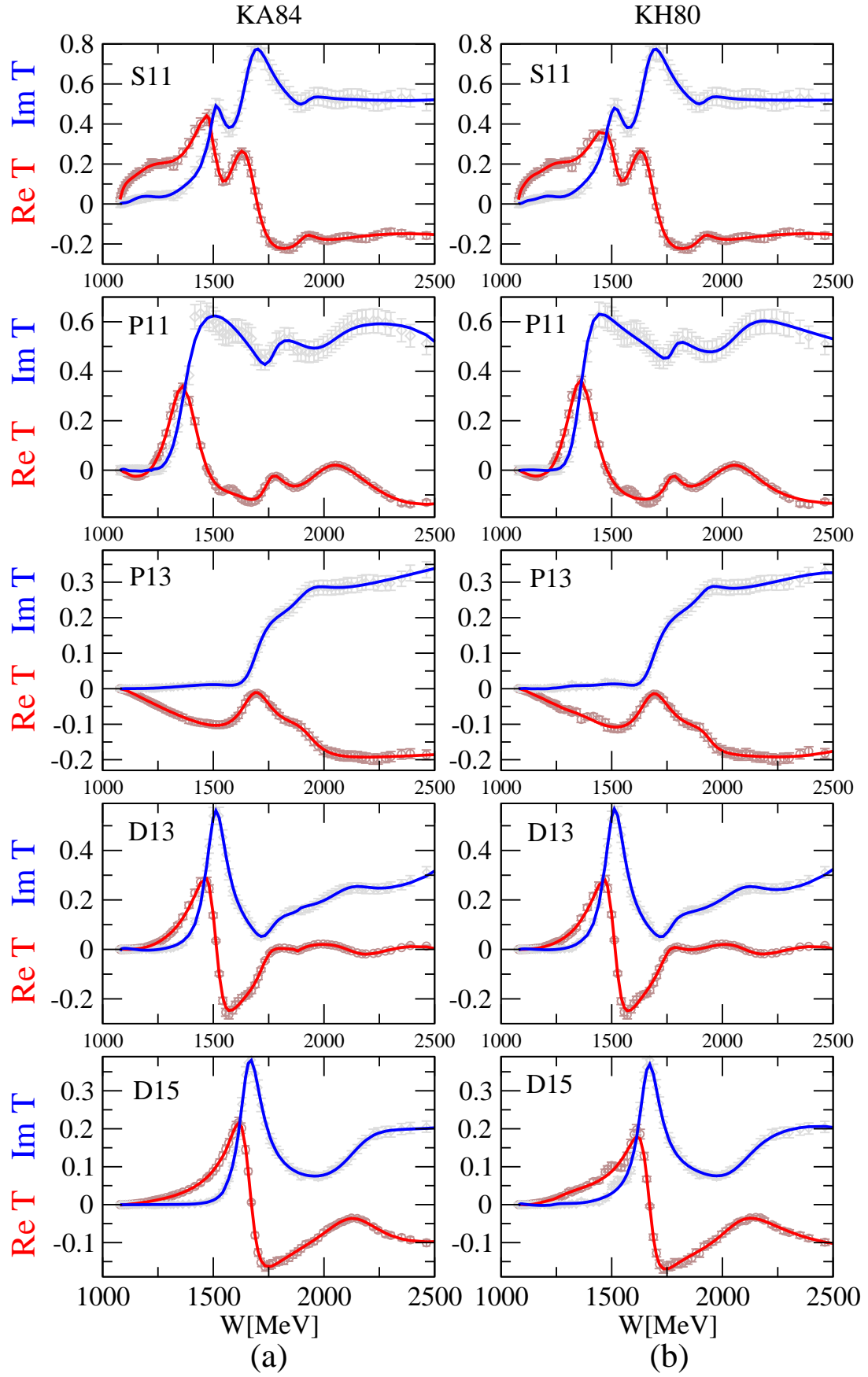


FIG. 1. (Color online) L+P fit for $I=1/2$ solutions, (a) Fit to KA84, (b) Fit to KH80.

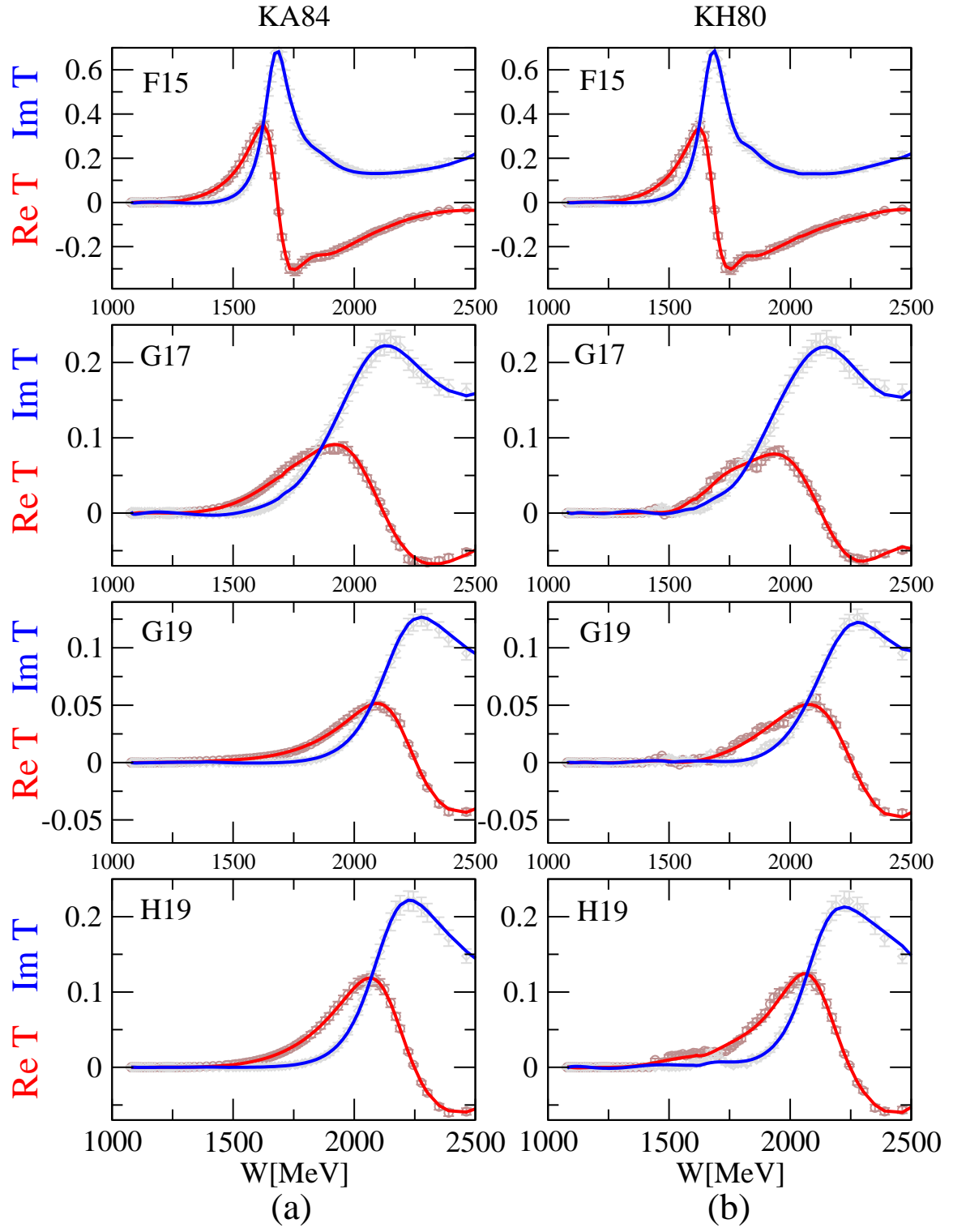


FIG. 2. (Color online) L+P fit for $I=1/2$ solutions, (a) Fit to KA84, (b) Fit to KH80.

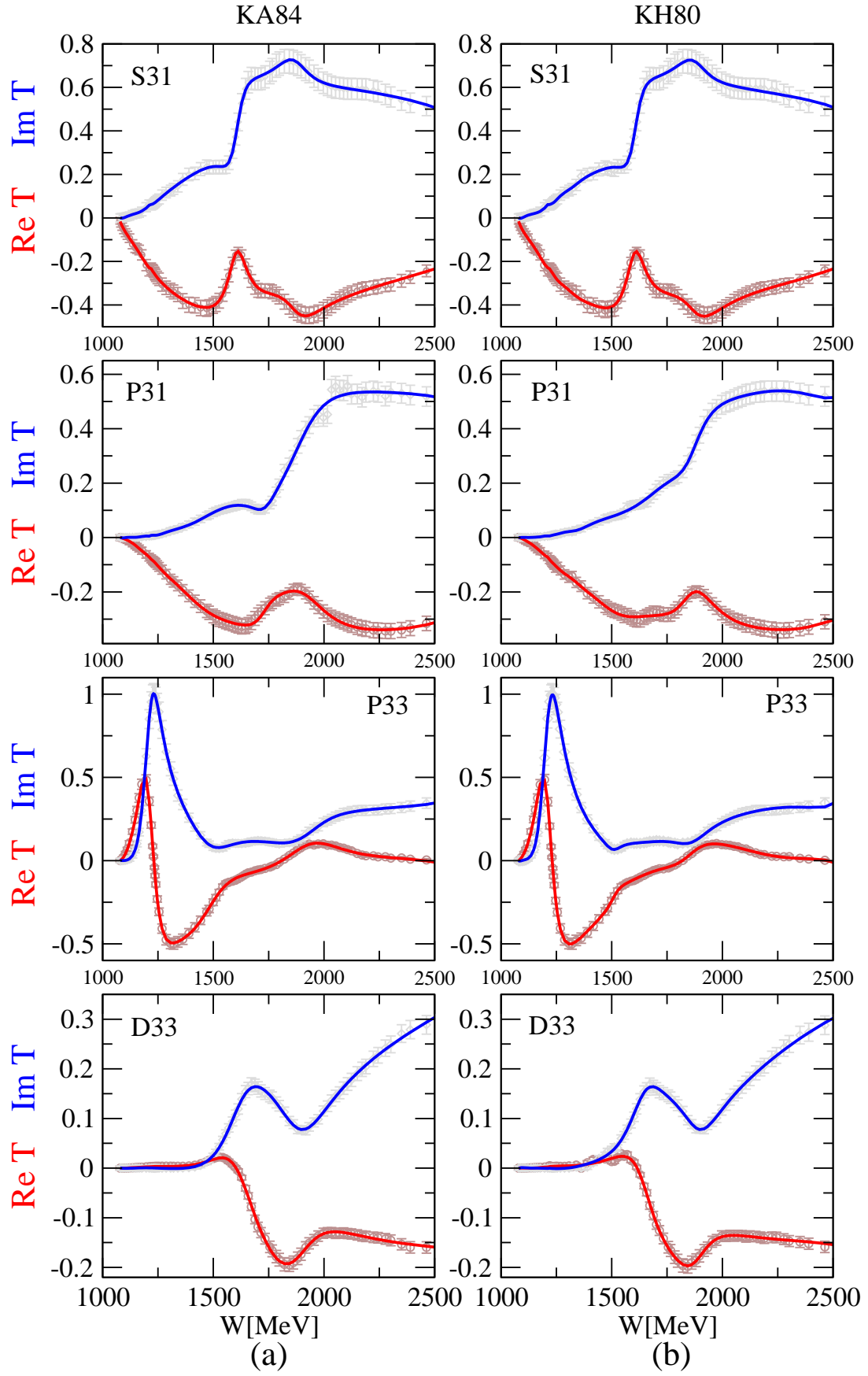


FIG. 3. (Color online) L+P fit for $I=3/2$ solutions, (a) Fit to KA84, (b) Fit to KH80.

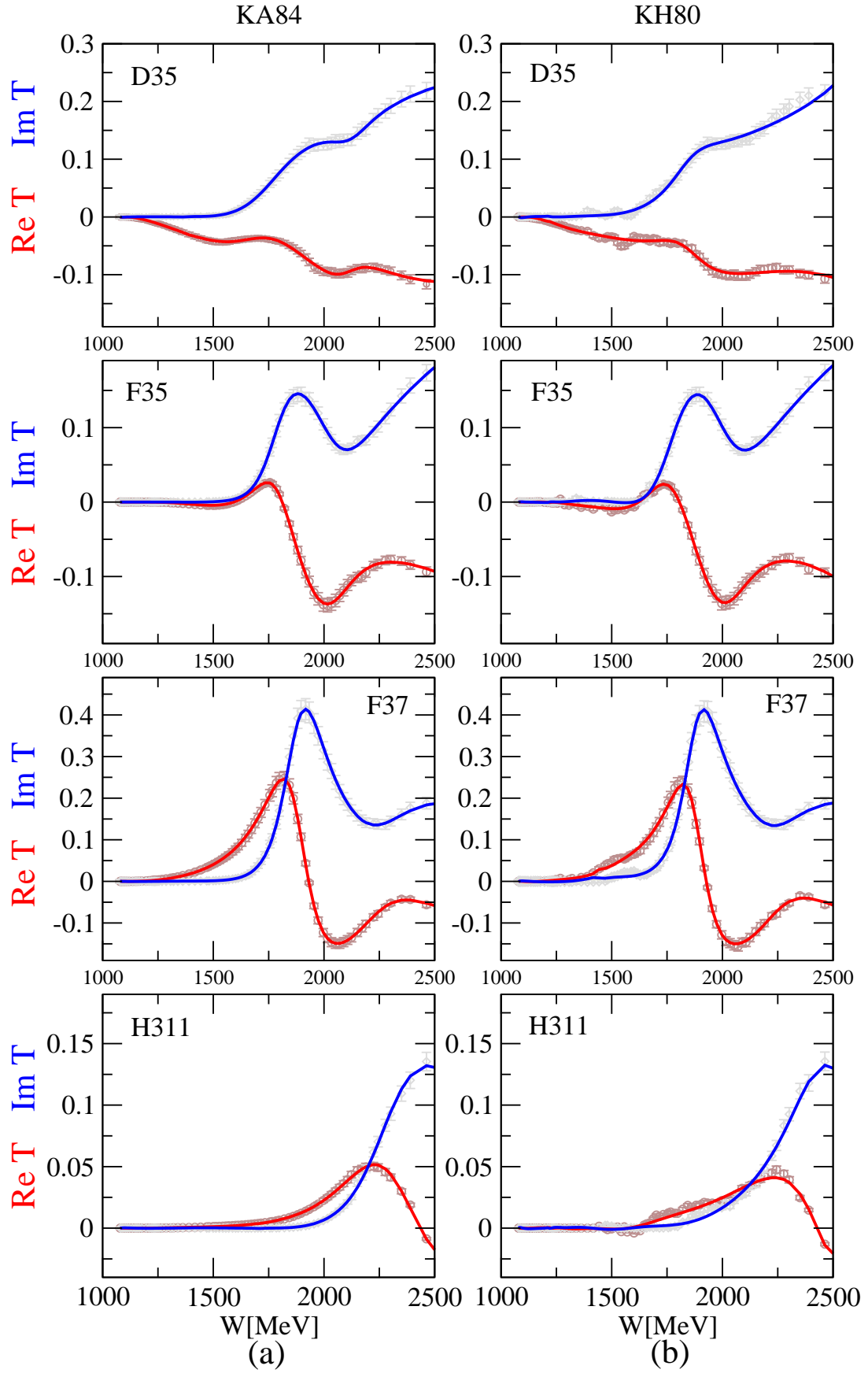


FIG. 4. (Color online) L+P fit for $I=3/2$ solutions, (a) Fit to KA84, (b) Fit to KH80.

TABLE III. Pole positions in MeV and residues of partial waves as moduli in MeV and phases in degrees for lowest $I = 3/2$ partial waves. The results from L+P expansion are given for Karlsruhe-Helsinki 80 (KH80) and Karlsruhe 84 (KA84) analyses. Resonances marked with a star indicate resonances which can be explained by ρ N complex branch point. RPP denotes the range of pole parameters given by Ref. [1], and RPP H93 denotes the values of pole parameters named HOEHLER 93 in RPP, and taken over from RPP and Table 1 of Ref. [5].

PW	Source	Resonance	$\text{Re } W_p$	$-2\text{Im } W_p$	residue	θ
S_{31}	RPP		1590 – 1610	120 – 140	13 – 20	(–110 ± 20)°
	RPP H93		1608	116	19	–95°
	KH80 L+P	$\Delta(1620) 1/2^-$	$1603 \pm 7 \pm 2$	$114 \pm 12 \pm 4$	$17 \pm 2 \pm 1$	$(-106 \pm 10 \pm 4)^\circ$
	KA84 L+P		$1605 \pm 5 \pm 2$	$108 \pm 9 \pm 1$	$16 \pm 0 \pm 1$	$(-103 \pm 6 \pm 3)^\circ$
	RPP		1820 – 1910 or 1780	130 – 345	10 ± 3	(–125 ± 20)° or (20 ± 40)°
	RPP H93		1780	–	–	–
	KH80 L+P	$\Delta(1900)^* 1/2^-$	$1865 \pm 35 \pm 19$	$187 \pm 50 \pm 19$	$11 \pm 4 \pm 2$	$(20 \pm 27 \pm 19)^\circ$
	KA84 L+P		$1867 \pm 22 \pm 9$	$191 \pm 23 \pm 7$	$12 \pm 0 \pm 2$	$(22 \pm 11 \pm 8)^\circ$
P_{31}	RPP		1830 – 1880	200 – 500	16 – 45	–
	RPP H93		1874	283	38	–
	KH80 L+P	$\Delta(1910) 1/2^+$	$1896 \pm 11 \pm 0$	$302 \pm 22 \pm 0$	$29 \pm 2 \pm 0$	$(-83 \pm 4 \pm 1)^\circ$
	KA84 L+P		$1880 \pm 19 \pm 11$	$325 \pm 37 \pm 16$	$30 \pm 4 \pm 1$	$(-97 \pm 7 \pm 9)^\circ$
	RPP		1209 – 1211	98 – 102	50 ± 3	(–46 ± 2)°
P_{33}	RPP H93		1209	100	50	–48°
	KH80 L+P	$\Delta(1232) 3/2^+$	$1211 \pm 1 \pm 1$	$98 \pm 2 \pm 1$	$50 \pm 1 \pm 1$	$(-46 \pm 1 \pm 1)^\circ$
	KA84 L+P		$1210 \pm 1 \pm 1$	$100 \pm 1 \pm 1$	$51 \pm 1 \pm 1$	$(-46 \pm 1 \pm 1)^\circ$
	RPP		1460 – 1560	200 – 350	5 – 44	–
	RPP H93		1550	–	–	–
	KH80 L+P	$\Delta(1600) 3/2^+$	$1469 \pm 10 \pm 5$	$314 \pm 18 \pm 8$	$38 \pm 2 \pm 2$	$(173 \pm 5 \pm 5)^\circ$
	KA84 L+P		$1489 \pm 9 \pm 2$	$289 \pm 17 \pm 6$	$31 \pm 3 \pm 2$	$(-174 \pm 5 \pm 3)^\circ$
	RPP		1850 – 1950	200 – 400	11 – 28	(–130 ± 30)° (–45 ± 30)°
	RPP H93		1900	–	–	–
	KH80 L+P	$\Delta(1920)^* 3/2^+$	$1906 \pm 10 \pm 2$	$310 \pm 20 \pm 11$	$26 \pm 3 \pm 2$	$-(130 \pm 5 \pm 3)^\circ$
	KA84 L+P		$1923 \pm 9 \pm 2$	$347 \pm 18 \pm 13$	$31 \pm 2 \pm 2$	$-(116 \pm 5 \pm 1)^\circ$
D_{33}	RPP		1620 – 1680	160 – 300	10 – 50	(–45 to 12)°
	RPP H93		1651	159	10	–
	KH80 L+P	$\Delta(1700) 3/2^-$	$1643 \pm 6 \pm 3$	$217 \pm 10 \pm 8$	$13 \pm 1 \pm 1$	$(-30 \pm 4 \pm 3)^\circ$
	KA84 L+P		$1616 \pm 3 \pm 2$	$280 \pm 6 \pm 3$	$21 \pm 1 \pm 1$	$(-58 \pm 2 \pm 2)^\circ$
	RPP		1900 – 2080	190 – 400	1 – 8	(135 ± 45)°
	RPP H93		–	–	–	–
	KH80 L+P	$\Delta(1940)^* 3/2^-$	$1878 \pm 11 \pm 5.5$	$212 \pm 21 \pm 6$	$9 \pm 1 \pm 1$	$(140 \pm 7 \pm 7)^\circ$
	KA84 L+P		$1884 \pm 7 \pm 2$	$303 \pm 13 \pm 8$	$18 \pm 1 \pm 1$	$(158 \pm 3 \pm 1)^\circ$
	RPP		1840 – 1960	175 – 360	7 – 30	(–20 ± 40)°
	RPP H93		1850	180	20	–
D_{35}	KH80 L+P	$\Delta(1930) 5/2^-$	$1848 \pm 9 \pm 19$	$321 \pm 17 \pm 7$	$9 \pm 1 \pm 1$	$(-37 \pm 3 \pm 7)^\circ$
	KA84 L+P		$1844 \pm 8 \pm 28$	$334 \pm 17 \pm 9$	$10 \pm 1 \pm 1$	$(-40 \pm 3 \pm 9)^\circ$

TABLE IV. Pole positions in MeV and residues of partial waves as moduli in MeV and phases in degrees for higher $I = 3/2$ partial waves. The results from L+P expansion are given for Karlsruhe-Helsinki 80 (KH80) and Karlsruhe 84 (KA84) analyses. RPP denotes the range of pole parameters given by Ref. [1], and RPP H93 denotes the values of pole parameters named HOEHLER 93 in RPP, and taken over from RPP and Table 1 of Ref. [5].

PW	Source	Resonance	$\text{Re } W_p$	$-2\text{Im } W_p$	$ \text{residue} $	θ
F_{35}	RPP		1805 – 1835	265 – 300	25 ± 10	(−50 ± 20)°
	RPP H93		1829	303	25	-
	KH80 L+P	$\Delta(1905) 5/2^+$	$1752 \pm 3 \pm 2$	$346 \pm 6 \pm 2$	$24 \pm 1 \pm 1$	$-(114 \pm 1 \pm 2)^\circ$
	KA84 L+P		$1790 \pm 3 \pm 2$	$293 \pm 6 \pm 6$	$19 \pm 1 \pm 1$	$-(77 \pm 2 \pm 2)^\circ$
	RPP		2000	250 – 450	16 ± 5	(150 ± 90)°
	RPP H93		–	–	–	–
	KH80 L+P	$\Delta(2000) 5/2^+$	$1998 \pm 4 \pm 4$	$404 \pm 10 \pm 4$	$34 \pm 1 \pm 1$	$(110 \pm 1 \pm 3)^\circ$
	KA84 L+P		$2035 \pm 6 \pm 6$	$381 \pm 13 \pm 20$	$23 \pm 1 \pm 3$	$(132 \pm 2 \pm 5)^\circ$
F_{37}	RPP		1870 – 1890	220 – 260	47 – 61	(−33 ± 12)°
	RPP H93		1878	230	47	−32°
	KH80 L+P	$\Delta(1950) 7/2^+$	$1877 \pm 2 \pm 1$	$223 \pm 4 \pm 1$	$44 \pm 1 \pm 0$	$-(39 \pm 1 \pm 1)^\circ$
	KA84 L+P		$1878 \pm 2 \pm 1$	$246 \pm 4 \pm 3$	$53 \pm 1 \pm 1$	$-(36 \pm 1 \pm 1)^\circ$
	RPP		2250 – 2350	160 – 360	12 ± 6	(−90 ± 60)°
	RPP H93		–	–	–	–
	KH80 L+P	$\Delta(2390) 7/2^+$	$2223 \pm 15 \pm 19$	$431 \pm 26 \pm 7$	$26 \pm 2 \pm 1$	$(-160 \pm 5 \pm 11)^\circ$
	KA84 L+P		$2257 \pm 13 \pm 8$	$472 \pm 25 \pm 20$	$30 \pm 2 \pm 2$	$(-131 \pm 4 \pm 3)^\circ$
H_{311}	RPP		2260 – 2400	350 – 750	12 – 39	−(30 ± 40)°
	RPP H93		2300	620	39	−60°
	KH80 L+P	$\Delta(2390) 11/2^+$	$2454 \pm 4 \pm 11$	$462 \pm 8 \pm 50$	$30 \pm 1 \pm 7$	$(11 \pm 1 \pm 8)^\circ$
	KA84 L+P		$2301 \pm 3 \pm 4$	$533 \pm 6 \pm 11$	$31 \pm 1 \pm 1$	$(-65 \pm 1 \pm 2)^\circ$

Taking into account arbitrariness of 2- vs 3-body solutions, we list resonances which are quite well established by the Karlsruhe-Helsinki analysis, and those which are only possible depending on the ratio of two-body to three-body final state. We have tried to fit with complex branch points and more resonances; however, without knowing the branching fraction of two-body to three-body, the complex branch point takes over the whole flux, and eliminates the additional resonance altogether.

TABLE V. Pole positions in MeV and residues of multipoles as moduli in $\text{mfm} \cdot \text{GeV}$ and phases in degrees. N_r is number of resonance poles. The results from L+P expansion are given for KH80 and KA84 solutions using ρN complex branch point.

Multipole	Source	N_r	Resonance	$\text{Re } W_p$	$-2\text{Im } W_p$	residue	θ	x_P	x_Q	x_R	D_{dp}
P_{11}	KH80 L+P	1	$N(1440) 1/2^+$	1368	167	45	-81°	369	$1077^{\pi N}$	$(1708 - i70)^{\rho N}$	0.325
	KA84 L+P	1		1372	170	43	-78°	277	$1077^{\pi N}$	$(1708 - i70)^{\rho N}$	0.354
P_{13}	KH80 L+P	1	$N(1720) 3/2^+$	1656	175	8	-151°	385	$1077^{\pi N}$	$(1708 - i70)^{\rho N}$	0.119
	KA84 L+P	1		1676	169	10	-105°	197	$1077^{\pi N}$	$(1708 - i70)^{\rho N}$	0.026
D_{13}	KH80 L+P	1	$N(1720) 3/2^-$	1506	119	34	-15°	784	$1077^{\pi N}$	$(1708 - i70)^{\rho N}$	0.154
	KA84 L+P	1		1507	114	32	-14°	756	$1077^{\pi N}$	$(1708 - i70)^{\rho N}$	0.161
D_{15}	KH80 L+P	1	$N(1675) 5/2^-$	1650	88	9	-24°	454	$1077^{\pi N}$	$(1708 - i70)^{\rho N}$	0.471
	KA84 L+P	1		1656	137	29	-30°	-644	$1077^{\pi N}$	$(1708 - i70)^{\rho N}$	0.058
F_{15}	KH80 L+P	1	$N(1680) 5/2^+$	1671	142	49	-22°	176	$1077^{\pi N}$	$(1708 - i70)^{\rho N}$	0.071
	KA84 L+P	1		1674	153	46	-23°	484	$1077^{\pi N}$	$(1708 - i70)^{\rho N}$	0.031
S_{31}	KH80 L+P	1	$\Delta(1620) 1/2^-$	1605	139	26	-109°	45	$1077^{\pi N}$	$(1708 - i70)^{\rho N}$	0.021
	KA84 L+P	1		1605	128	21	-107°	-2446	$1077^{\pi N}$	$(1708 - i70)^{\rho N}$	0.018
P_{31}	KH80 L+P	1	$\Delta(1910) 1/2^+$	1847	257	49	-128°	739	$1077^{\pi N}$	$(1708 - i70)^{\rho N}$	0.109
	KA84 L+P	1		1891	398	40	-75°	-203	$1077^{\pi N}$	$(1708 - i70)^{\rho N}$	0.025
	KH80 L+P	0	-	-	-	-	-	-556	$1077^{\pi N}$	$(1708 - i70)^{\rho N}$	0.123
	KA84 L+P	0	-	-	-	-	-	404	$1077^{\pi N}$	$(1708 - i70)^{\rho N}$	0.040
P_{33}	KH80 L+P	2	$\Delta(1232) 3/2^+$	1210	102	53	-47°	656	$1077^{\pi N}$	$(1708 - i70)^{\rho N}$	0.025
			$\Delta(1600) 3/2^+$	1537	157	10	-105°				
	KA84 L+P	2	$\Delta(1232) 3/2^+$	1210	102	53	-47°	-403	$1077^{\pi N}$	$(1708 - i70)^{\rho N}$	0.034
			$\Delta(1600) 3/2^+$	1545	155	10	-95°				
D_{33}	KH80 L+P	1	$\Delta(1700) 3/2^+$	1663	180	12	15	53	$1077^{\pi N}$	$(1708 - i70)^{\rho N}$	0.161
	KA84 L+P	1		1574	373	29	-111°	69	$1077^{\pi N}$	$(1708 - i70)^{\rho N}$	0.034
D_{35}	KH80 L+P	1	$\Delta(1930) 5/2^-$	1813	242	8	-72°	-302	$1077^{\pi N}$	$(1708 - i70)^{\rho N}$	0.498
	KA84 L+P	1		1889	258	16	-49°	-2398	$1077^{\pi N}$	$(1708 - i70)^{\rho N}$	0.069
	KH80 L+P	0	-	-	-	-	-	887	$1077^{\pi N}$	$(1708 - i70)^{\rho N}$	0.303
	KA84 L+P	0	-	-	-	-	-	24	$1077^{\pi N}$	$(1708 - i70)^{\rho N}$	0.102
F_{35}	KH80 L+P	2	$\Delta(1905) 5/2^+$	1782	243	17	-162°	899	$1077^{\pi N}$	$(1708 - i70)^{\rho N}$	0.254
			$\Delta(2000) 5/2^+$	2027	449	39	137°				
	KA84 L+P	2	$\Delta(1905) 5/2^+$	1790	314	22	-76°	-240	$1077^{\pi N}$	$(1708 - i70)^{\rho N}$	0.045
			$\Delta(2000) 5/2^+$	2035	408	27	135°				
F_{37}	KH80 L+P	2	$\Delta(1950) 7/2^+$	1893	275	65	-15°	802	$1077^{\pi N}$	$(1708 - i70)^{\rho N}$	0.204
			$\Delta(2390) 7/2^+$	2419	323	16	-27°				
	KA84 L+P	2	$\Delta(1950) 7/2^+$	1882	252	54	-31°	520	$1077^{\pi N}$	$(1708 - i70)^{\rho N}$	0.021
			$\Delta(2390) 7/2^+$	2311	469	31	-100°				

IV. DISCUSSION AND CONCLUSIONS

Using the L+P method we obtain almost perfect fits to all KH80 and KA84 partial waves. This is visible in very low discrepancy parameters D_{dp} given in Tables VI and VII, and in excellent visual agreement of fitting curves and input data in Figs. 1 - 4. Agreement is somewhat poorer for KH80 H_{311} , G_{17} and G_{19} partial waves. For the first one, the discrepancy parameter is of the order of 2-3, while for the latter two it is of order 1. For all other partial waves it is significantly below one. However, these results are consistent with the graphs in Fig. 1 - 4. A closer look at the KH80 $H_{3,11}$ partial wave in Fig. 4, one can detect somewhat poorer agreement of the real part of the fitted curve with data near 1700 and 2100 MeV, and for imaginary parts near 1900 MeV. Similar discrepancies can be found for G_{17} and G_{19} partial waves if Fig. 2 is closely inspected. Such exceptions are not present for the KA84 solution. All partial waves for KA84 are fitted with discrepancy parameters significantly below one. This supports the statement given in [5] that the KA84 solution is obtained by further smoothing of the KH80 solution, and the L+P method can fit KA84 slightly better than KH80 due to additional smoothing.

We confirm the values of all the pole positions of the Karlsruhe-Helsinki solutions given in the RPP using the speed plot method of Ref [5] for the KA84 solution with better precision and confidence, giving corresponding solutions for the same resonances of the KH80 solution, and a number of new poles which all agree with results quoted in the RPP.

The new resonances, in the RPP but not established by the SP method are: $S_{11} N(1895)1/2-$, $P_{11} N(2100)1/2+$, $P_{13} N(1900)3/2+$, $D_{13} N(1875)3/2-$, $F_{15} N(2000)5/2+$, $D_{33} \Delta(1940)3/2-$, $F_{35} \Delta(2000)5/2+$ and $F_{37} \Delta(2390)7/2+$.

We confirm that visual shapes of KH80 and KA84 solutions and numerical values of pole positions are very similar, and in practice either solution can be used. Masses (real parts) of KH80 and KA84 poles are within error bars; however some partial waves (the first $D_{33} \Delta(1700)3/2-$ and first $F_{35} \Delta(1905) 5/2+$) show slightly more than one standard deviation discrepancy when the widths (imaginary parts) of poles are compared. Others are within one standard deviation.

We establish that any single-channel model based solely on one channel of input data (in our case Karlsruhe-Helsinki PWA), is unable to distinguish between alternative two-body and three-body final state solutions. The L+P model can produce equivalent solutions for two-body and three-body final states; without new data, the two-body to three-body branching fraction remains undetermined. In Tables I, II, III and IV we denote with asterisks solutions which have the same discrepancy ratio, but realized through different physics formalisms: two-body final state given with real branch point or three-body final state given by complex branch point. All these solutions are indistinguishable within single-channel models.

It is very interesting to observe that we have even more ambiguity in the L+P method. There are partial waves in which the L+P method gives equivalent solutions in three-body formalism with one resonance or without any resonances at all. These are: P_{31} and D_{35} partial waves (see Table V).

What is important is that the dominant resonances in two-body or three-body formalism have identical parameters; i.e. the single channel formalism *without ambiguity* establishes the existence of resonances without an asterisk.

The three-body formalism using complex branch points raises some doubt about higher order resonances, and requires measurement of new data for inelastic channels. Only firm experimental numbers on inelastic 2-body \rightarrow 2-body or higher energy 2-body \rightarrow 3-body data can resolve the ambiguity between solutions given by single-channel analysis. We endorse strongly any new proposal which plans to measure inelastic $\pi N \rightarrow XY$ channels, e.g. [25].

ACKNOWLEDGMENT

Many thanks go to David Bugg who carefully read the manuscript, significantly improved English fluency, and helped this paper to attain its final form. This work was supported in part by Tuzla Canton, Bosnia and Herzegovina, Ministry of Education, Science, Culture and Sport grant 10/1-14-020637-1/13.

APPENDIX

TABLE VI. Parameters from L+P expansion are given for KH80 solution. N_r is number of resonance poles, x_P, x_Q, x_R are branch points in MeV.

Source KH80											
PW	N_r	x_P	x_Q	x_R	D_{dp}	PW	N_r	x_P	x_Q	x_R	D_{dp}
S_{11}	3	-18216	$1077^{\pi N}$	$1215^{\pi\pi N}$	0.131	S_{31}	2	-1123	$1077^{\pi N}$	$1215^{\pi\pi N}$	0.036
	3	779	$1077^{\pi N}$	$1486^{\eta N}$	0.130		2	-1967	$1077^{\pi N}$	$1370^{Real(\pi\Delta)}$	0.043
	3	-2529	$1077^{\pi N}$	1491^{free}	0.127		2	900	$1077^{\pi N}$	$1708^{Real(\rho N)}$	0.041
							2	-1239	$1077^{\pi N}$	1702^{free}	0.035
P_{11}	3	-1135	$1077^{\pi N}$	$1215^{\pi\pi N}$	0.408	P_{31}	1	314	$1077^{\pi N}$	$1215^{\pi\pi N}$	0.0789
	3	-1270	$1077^{\pi N}$	$1370^{Real(\pi\Delta)}$	0.453		1	281	$1077^{\pi N}$	1210^{free}	0.0786
	3	-1988	$1077^{\pi N}$	1320^{free}	0.474						
P_{13}	2	-28412	$1077^{\pi N}$	$1215^{\pi\pi N}$	0.126	P_{33}	3	215	$1077^{\pi N}$	$1215^{\pi\pi N}$	0.098
	2	776	$1077^{\pi N}$	$1370^{Real(\pi\Delta)}$	0.119		3	707	$1077^{\pi N}$	$1370^{Real(\pi\Delta)}$	0.097
	2	-617	$1077^{\pi N}$	1267	0.118		3	898	$1077^{\pi N}$	1378^{free}	0.076
D_{13}	3	-697	$1077^{\pi N}$	$1215^{\pi\pi N}$	0.230	D_{33}	2	-3832	$1077^{\pi N}$	$1215^{\pi\pi N}$	0.178
	3	-4763	$1077^{\pi N}$	$1370^{Real(\pi\Delta)}$	0.278		2	-3104	$1077^{\pi N}$	$1370^{Real(\pi\Delta)}$	0.095
	3	-8507	$1077^{\pi N}$	$1708^{Real(\rho N)}$	0.236		2	-14033	$1077^{\pi N}$	1362^{free}	0.094
	3	-2066	$1077^{\pi N}$	1107^{free}	0.224						
D_{15}	2	407	$1077^{\pi N}$	$1215^{\pi\pi N}$	0.536	D_{35}	1	315	$1077^{\pi N}$	$1215^{\pi\pi N}$	0.576
	2	223	$1077^{\pi N}$	$1370^{Real(\pi\Delta)}$	0.525		1	331	$1077^{\pi N}$	$1688^{K\Sigma}$	0.578
	2	-5667	$1077^{\pi N}$	1511^{free}	0.469		1	409	$1077^{\pi N}$	1211^{free}	0.576
F_{15}	2	239	$1077^{\pi N}$	$1215^{\pi\pi N}$	0.136	F_{35}	2	7.8	$1077^{\pi N}$	$1215^{\pi\pi N}$	0.343
	2	43.9	$1077^{\pi N}$	$1370^{Real(\pi\Delta)}$	0.124		2	-249	$1077^{\pi N}$	$1708^{Real(\rho N)}$	0.344
	2	-157	$1077^{\pi N}$	$1708^{Real(\rho N)}$	0.108		2	98	$1077^{\pi N}$	1221^{free}	0.330
	2	-14.1	$1077^{\pi N}$	1673^{free}	0.105						
G_{17}	1	-261	$1077^{\pi N}$	$1215^{\pi\pi N}$	1.211	F_{37}	2	-324	$1077^{\pi N}$	$1370^{Real(\pi\Delta)}$	0.376
	1	298	$1077^{\pi N}$	$1486^{\eta N}$	1.302		2	-439	$1077^{\pi N}$	$1708^{Real(\rho N)}$	0.379
	1	-148	$1077^{\pi N}$	1445^{free}	1.164		2	-141	$1077^{\pi N}$	1463^{free}	0.374
G_{19}	1	-10490	$1077^{\pi N}$	$1486^{\eta N}$	1.835	H_{311}	1	-35183	$1077^{\pi N}$	$1215^{\pi\pi N}$	3.513
	1	-838	$1077^{\pi N}$	$1611^{K\Lambda}$	1.025		1	-1460	$1077^{\pi N}$	$1688^{K\Sigma}$	3.009
	1	-196	$1077^{\pi N}$	1713^{free}	0.975		1	87.7	$1077^{\pi N}$	1489^{free}	2.482
H_{19}	1	-49	$1077^{\pi N}$	$1486^{\eta N}$	0.315						
	1	-1093	$1077^{\pi N}$	$1611^{K\Lambda}$	0.492						
	1	-1252	$1077^{\pi N}$	1709^{free}	0.298						

TABLE VII. Parameters from L+P expansion are given for KA84 solution. N_r is number of resonance poles, x_P, x_Q, x_R are branch points in MeV.

Source KA84											
PW	N_r	x_P	x_Q	x_R	D_{dp}	PW	N_r	x_P	x_Q	x_R	D_{dp}
S_{11}	3	822	$1077^{\pi N}$	$1215^{\pi\pi N}$	0.159	S_{31}	2	-521	$1077^{\pi N}$	$1215^{\pi\pi N}$	0.034
	3	900	$1077^{\pi N}$	$1486^{\eta N}$	0.105		2	663	$1077^{\pi N}$	$1370^{Real(\pi\Delta)}$	0.039
	3	900	$1077^{\pi N}$	1499^{free}	0.096		2	196	$1077^{\pi N}$	$1708^{Real(\rho N)}$	0.037
								-255	$1077^{\pi N}$	1217^{free}	0.033
P_{11}	3	287	$1077^{\pi N}$	$1215^{\pi\pi N}$	0.459	P_{31}	1	-690	$1077^{\pi N}$	$1215^{\pi\pi N}$	0.091
	3	-7351	$1077^{\pi N}$	$1370^{Real(\pi\Delta)}$	0.451		1	-658	$1077^{\pi N}$	1221^{free}	0.088
	3	-2082	$1077^{\pi N}$	1382^{free}	0.377						
P_{13}	2	345	$1077^{\pi N}$	$1215^{\pi\pi N}$	0.037	P_{33}	3	440	$1077^{\pi N}$	$1215^{\pi\pi N}$	0.081
	2	-957	$1077^{\pi N}$	$1370^{Real(\pi\Delta)}$	0.038		3	576	$1077^{\pi N}$	$1370^{Real(\pi\Delta)}$	0.088
	2	543	$1077^{\pi N}$	1201^{free}	0.036		3	-646	$1077^{\pi N}$	1469^{free}	0.076
D_{13}	3	-0.024	$1077^{\pi N}$	$1215^{\pi\pi N}$	0.332	D_{33}	2	-696	$1077^{\pi N}$	$1215^{\pi\pi N}$	0.066
	3	-1567	$1077^{\pi N}$	$1370^{Real(\pi\Delta)}$	0.331		2	-31769	$1077^{\pi N}$	$1370^{Real(\pi\Delta)}$	0.063
	3	-758	$1077^{\pi N}$	$1708^{Real(\rho N)}$	0.270		2	-27693	$1077^{\pi N}$	1362^{free}	0.061
	3	-1449	$1077^{\pi N}$	1880^{free}	0.249						
D_{15}	2	753	$1077^{\pi N}$	$1215^{\pi\pi N}$	0.069	D_{35}	1	-3753	$1077^{\pi N}$	$1215^{\pi\pi N}$	0.062
	2	-4045	$1077^{\pi N}$	$1370^{Real(\pi\Delta)}$	0.070		1	271	$1077^{\pi N}$	$1688^{K\Sigma}$	0.063
	2	-5667	$1077^{\pi N}$	1547^{free}	0.057		1	409	$1077^{\pi N}$	1382^{free}	0.060
F_{15}	2	-139	$1077^{\pi N}$	$1215^{\pi\pi N}$	0.084	F_{35}	2	-1063	$1077^{\pi N}$	$1215^{\pi\pi N}$	0.045
	2	-0.047	$1077^{\pi N}$	$1370^{Real(\pi\Delta)}$	0.081		2	-3331	$1077^{\pi N}$	$1708^{Real(\rho N)}$	0.057
	2	-332	$1077^{\pi N}$	$1708^{Real(\rho N)}$	0.052		2	-1384	$1077^{\pi N}$	1186^{free}	0.044
	2	546	$1077^{\pi N}$	1361^{free}	0.027						
G_{17}	1	-50	$1077^{\pi N}$	$1215^{\pi\pi N}$	0.354	F_{37}	2	-4046	$1077^{\pi N}$	$1370^{Real(\pi\Delta)}$	0.039
	1	-1513	$1077^{\pi N}$	$1486^{\eta N}$	0.453		2	-3041	$1077^{\pi N}$	$1708^{Real(\rho N)}$	0.039
	1	250	$1077^{\pi N}$	1307^{free}	0.351		2	-3167	$1077^{\pi N}$	1903^{free}	0.027
G_{19}	1	-1459	$1077^{\pi N}$	$1486^{\eta N}$	0.345	H_{311}	1	-983	$1077^{\pi N}$	$1215^{\pi\pi N}$	0.136
	1	-2385	$1077^{\pi N}$	$1611^{K\Lambda}$	0.556		1	-1099	$1077^{\pi N}$	$1688^{K\Sigma}$	0.142
	1	194	$1077^{\pi N}$	1406^{free}	0.115		1	44	$1077^{\pi N}$	1462^{free}	0.107
H_{19}	1	-378	$1077^{\pi N}$	$1486^{\eta N}$	0.027						
	1	433	$1077^{\pi N}$	$1611^{K\Lambda}$	0.021						
	1	556	$1077^{\pi N}$	1715^{free}	0.019						

-
- [1] J. Beringer et al. (Particle Data Group), Phys. Rev. **D86**, 010001 (2012).
 - [2] International Workshop on NEW PARTIAL WAVE ANALYSIS TOOLS FOR NEXT GENERATION HADRON SPECTROSCOPY EXPERIMENTS, June 20-22, 2012, Camogli, Italy. [www.ge.infn.it/~athos12].
 - [3] ATHOS 2013-International Workshop on New Partial Wave Analysis Tools for Next-Generation Hadron Spectroscopy Experiments, 21-24 May 2013 Kloster Seeon, Germany.
 - [4] 7th International Workshop on Pion-Nucleon Partial Wave Analysis and the Interpretation of Baryon Resonances (PWA7), 23-27 September 2013, Camogli, Italy.
 - [5] G. Höhler, π N Newsletter **9**, 1 (1993).
 - [6] G. Höhler and A. Schulte, π N Newsletter, **7**, 94, (1992).
 - [7] G. Höhler, NSTAR 2001: Proceedings of the Workshop on the Physics of Excited Nucleons; Mainz, Germany, 7-10 March 2001, World Scientific, 2001, ed. D. Drechsel and L. Tiator, Pg.185.
 - [8] A. Švarc, M. Hadžimehmedović, H. Osmanović, and J. Stahov, arXiv:1212.1295 [nucl-th].
 - [9] A. Švarc, M. Hadžimehmedović, H. Osmanović, J. Stahov, L. Tiator, R. L. Workman, Phys. Rev. **C 88**, 035206 (2013).
 - [10] S. Ceci, J. Stahov, A. Švarc, S. Watson, and B. Zauner, Phys. Rev. **D 77**, 116007 (2008).
 - [11] P. Masjuan, J.J. Sanz-Cillero, Eur.Phys.J. **C73** (2013) 2594.
 - [12] R. L. Kelly, and R. E. Cutkosky, Phys. Rev. **D 20**, 2782 (1979).
 - [13] R. E. Cutkosky, R. E. Hendrick, J. W. Alcock, Y. A. Chao, R. G. Lipes, J. C. Sandusky, and R. L. Kelly, Phys. Rev. **D 20**, 2804 (1979).
 - [14] R. E. Cutkosky, C. P. Forsyth, R. E. Hendrick, and R. L. Kelly, Phys. Rev. **D 20**, 2839 (1979).
 - [15] G. Höhler, *Pion Nucleon Scattering*, Part 2, Landolt-Bornstein: Elastic and Charge Exchange Scattering of Elementary Particles, Vol. 9b (Springer-Verlag, Berlin, 1983).
 - [16] R. Koch, Z. Physik **C 29**, 597 (1985) and R. Koch; M. Sararu, Karlsruhe Report **TKP84-6** (1984) and R. Koch: Nucl. Phys. **A448**, 707 (1986).
 - [17] G. Höhler et al., Karlsruhe report TKP 83-24 (1983)
 - [18] Michiel Hazewinkel: *Encyclopaedia of Mathematics*, Vol.6, Springer, 31. 8. 1990, pg.251.
 - [19] S. Ciulli and J. Fischer, Nucl. Phys. **24**, 465 (1961).
 - [20] I. Ciulli, S. Ciulli, and J. Fisher, Nuovo Cimento **23**, 1129 (1962).
 - [21] E. Pietarinen, Nuovo Cimento **12A**, 522 (1972).
 - [22] C. G. Boyd, B. Grinstein, and R. F. Lebed, Phys.Rev.Lett. **74**, 4603 (1995); R. J. Hill, and G. Paz, Phys. Rev. **D 82**, 113005 (2010).
 - [23] S. Ceci, M. Döring, C. Hanhart, S. Krewald, U.-G. Meissner, and A. Švarc, Phys. Rev. **C 84**, 015205 (2011).
 - [24] D. Rönchen, M. Döring, F. Huang, H. Haberzettl, J. Haidenbauer, C. Hanhart, S. Krewald, U.-G. Meissner, and K. Nakayama, Eur. Phys. J. **A 49**, 44 (2013).
 - [25] K.H. Hicks, et al., Proposal for J-PARC 50 GeV Proton Synchrotron, 2013, <https://www.dropbox.com/s/radetvyly2qhfbe/JPARC-hybrid-baryon-proposal-v2.pdf>.